

# Narrow $J^\pi = 1/2^+, 3/2^+, \text{ and } 3/2^-$ states of $\Theta^+$ in a Quark model with Antisymmetrized Molecular Dynamics

Y. Kanada-En'yo, O. Morimatsu, and T. Nishikawa

*Institute of Particle and Nuclear Studies,  
High Energy Accelerator Research Organization,  
1-1 Oho, Tsukuba, Ibaraki 305-0801, Japan*

The exotic baryon  $\Theta^+(uudd\bar{s})$  is studied with microscopic calculations in a quark model by using a method of antisymmetrized molecular dynamics. We predict that three narrow states,  $J^\pi = 1/2^+(I = 0)$ ,  $J^\pi = 3/2^+(I = 0)$ , and  $J^\pi = 3/2^-(I = 1)$  nearly degenerate with the lowest  $1/2^-$  state in the  $uudd\bar{s}$  system. We discuss  $KN$  decay widths and estimate them to be  $\Gamma < 7$  for the  $J^\pi = \{1/2^+, 3/2^+\}$ , and  $\Gamma < 1$  MeV for the  $J^\pi = 3/2^-$  state. In contrast to these narrow states, the  $1/2^-$  states should be much broader. We assign the observed  $\Theta^+$  as the  $J^\pi = \{1/2^+, 3/2^+\}$ .

## I. INTRODUCTION

The exotic baryon  $\Theta^+$  has recently been reported by several experimental groups [1–9]. Since the quantum numbers determined from its decay modes indicate that the minimal quark content is  $uudd\bar{s}$ , these induced experimental and theoretical studies of multi-quark hadrons. However it should be kept in mind that the  $\Theta^+$  has not been well established yet because of the low statistics and experimental reports [10–12] for no evidence of the  $\Theta^+$ .

The prediction of a  $J^\pi = 1/2^+$  state of  $uudd\bar{s}$  by a chiral soliton model [13] motivated the experiments of the first observation of  $\Theta^+$  [1]. Their prediction of even parity is unnatural in the naive quark model, because the lowest  $q^4\bar{q}$  state is expected to be spatially symmetric and have odd parity due to the odd intrinsic parity of the anti-quark. Theoretical studies were done to describe  $\Theta^+$  by many groups [14–21], some of which predicted the opposite parity,  $J^\pi = 1/2^-$  [18–20]. The problem of spin and parity of  $\Theta^+$  is not only open but also essential to understand the dynamics of pentaquark systems. To solve this problem, it is crucial to calculate five-quark system relying on less *a priori* assumptions such as the existence of quark clusters or the spin parity.

In this paper we would like to clarify the mechanism of the existence of the pentaquark baryon and predict possible narrow  $\Theta^+$  states. We try to extract a simple picture for the pentaquark baryon with its energy, width, spin, parity and also its shape from explicit 5-body calculation. In order to achieve this goal, we study the pentaquark with a flux-tube model [24,25] based on strong coupling QCD, by using a method of antisymmetrized molecular dynamics (AMD) [22,23]. In the flux-tube model, the interaction energy of quarks and anti-quarks is given by the energy of the string-like color-electric flux, which is proportional to the minimal length of the flux-tube connecting quarks and anti-quarks at long distances supplemented by perturbative one-gluon-exchange (OGE) interaction at short distances. For the  $q^4\bar{q}$  system the flux-tube configuration has an exotic topology, Fig.1(c), in addition to an ordinary meson-baryon topology, Fig. 1(d), and the transition between different topologies takes place only in higher order of the strong coupling expansion. Therefore, it seems quite natural that the flux-tube model accommodates the pentaquark baryon. In 1991, Carlson and Pandharipande studied exotic hadrons in the flux-tube model [26]. They calculated for only a few  $q^4\bar{q}$  states with very limited quantum numbers and concluded that pentaquark baryons are absent. We apply the AMD method to the flux-tube model. The AMD is a variational method to solve a finite many-fermion system. This method is powerful for the study of nuclear structure. One of the advantages of this method is that the spatial and spin degrees of freedom for all particles are independently treated. This method can successfully describe various types of structure such as shell-model-like structure and clustering (correlated nucleons) in nuclear physics. In the application of this method to a quark model, we take the dominant terms of OGE potential and string potential due to the gluon flux tube. Different flux-tube configurations are assumed to be decoupled. Since we are interested in the narrow states, we only adopt the confined configuration given by Fig.1(c). We calculate all the possible spin parity states of  $uudd\bar{s}$  system, and predict low-lying states. By analysing the wave function, we discuss the properties of  $\Theta^+$  and estimate the decay widths of these states with a method of reduced width amplitudes.

This paper is organized as follows. We explain the formulation of the present framework in the next section, and show the results in III. In IV, we discuss the structure of low-lying states and their widths. Finally, we give a summary in V.

## II. FORMULATION

In the present calculation, the quarks are treated as non-relativistic spin- $\frac{1}{2}$  Fermions. We use a Hamiltonian as follows,

$$H = H_0 + H_I + H_f, \quad (1)$$

where  $H_0$  is the kinetic energy of the quarks,  $H_I$  represents the short-range OGE interaction between the quarks and  $H_f$  is the energy of the flux tubes. For simplicity, we take into account the mass difference between the  $ud$  quarks and the  $s$  quark, only in the mass term of  $H_0$  but not in the kinetic energy term. Then,  $H_0$  is represented as follows;

$$H_0 = \sum_i^{N_q} m_i + \sum_i^{N_q} \frac{p_i^2}{2m_q} - T_0, \quad (2)$$

where  $N_q$  is the total number of quarks and  $m_i$  is the mass of  $i$ -th quark, which is  $m_q$  for a  $u$  or  $d$  quark and  $m_s$  for a  $\bar{s}$  quark.  $T_0$  denotes the kinetic energy of the center-of-mass motion.

$H_I$  represents the short-range OGE interaction between quarks and consists of the Coulomb and the color-magnetic terms,

$$H_I = \alpha_c \sum_{i < j} F_i F_j \left[ \frac{1}{r_{ij}} - \frac{2\pi}{3m_i m_j} s(r_{ij}) \sigma_i \cdot \sigma_j \right]. \quad (3)$$

Here,  $\alpha_c$  is the quark-gluon coupling constant, and  $F_i F_j$  is defined by  $\sum_{\alpha=1,\dots,8} F_i^\alpha F_j^\alpha$ , where  $F_i^\alpha$  is the generator of color  $SU(3)$ ,  $\frac{1}{2}\lambda_i^\alpha$  for quarks and  $-\frac{1}{2}(\lambda_i^\alpha)^*$  for anti-quarks. The usual  $\delta(r_{ij})$  function in the spin-spin interaction is replaced by a finite-range Gaussian,  $s(r_{ij}) = \left[ \frac{1}{2\sqrt{\pi}\Lambda} \right]^3 \exp \left[ -\frac{r_{ij}^2}{4\Lambda^2} \right]$ , as in Ref. [26]. Of course, the full OGE interaction contains other terms such as tensor and spin-orbit interactions. However, since our main interest here is to see the basic properties of the pentaquark, we do not include these minor contributions.

In the flux-tube quark model [24], the confining string potential is written as  $H_f = \sigma L_f - M^0$ , where  $\sigma$  is the string tension,  $L_f$  is the minimum length of the flux tubes, and  $M^0$  is the zero-point string energy.  $M^0$  depends on the topology of the flux tubes and is necessary to fit the  $q\bar{q}$ ,  $q^3$  and  $q^4\bar{q}$  potential obtained from lattice QCD or phenomenology. In the present calculation, we adjust the  $M^0$  to fit the absolute masses for each of three-quark and pentaquark.

For the meson and  $3q$ -baryon systems, the flux-tube configurations are the linear line and the  $Y$ -type configuration with three bonds and one junction as shown in Fig.2(a) and (b), respectively. The string potential given by the  $Y$ -type flux tube in a  $3q$ -baryon system is supported by Lattice QCD [27]. For the pentaquark system, the different types of flux-tube configurations appear as shown in Fig. 1.(e),(f), and (d), which correspond to the states,  $|\Phi_{(e)}\rangle = |[ud][ud]\bar{s}\rangle$ ,  $|\Phi_{(f)}\rangle = |[uu][dd]\bar{s}\rangle$ , and  $|\Phi_{(d)}\rangle = |(qqq)_1(qq)_1\rangle$ , respectively. ( $[qq]$  is defined by color anti-triplet of  $qq$ .) The flux-tube configuration (e) or (f) have seven bonds and three junctions, while the configuration (d) has four bonds and one junction. In principle, besides these color configurations ( $[qq][qq]\bar{q}$  and  $(qqq)_1(qq)_1$ ), other color configurations are possible in totally color-singlet  $q^4\bar{q}$  systems by incorporating a color-symmetric  $(qq)_6$  pair as in Refs. [16,21]. However, since such a string from the  $(qq)_6$  is energetically excited and is disfavored in the strong coupling limit of gauge theories as shown in Ref. [28]. Therefore, we consider only color-3 flux tubes as the elementary tubes. In fact, the string tension for the color-6 string in the strong coupling limit is 5/2 times larger than that for the color-3 string from the expectation value of the Casimir operator. The string potentials given by the tube lengths of the configuration Fig.1(c) is supported by Lattice QCD calculations [29].

In the present calculation of the energy, we neglect the transition among  $|\Phi_{(e)}\rangle$ ,  $|\Phi_{(f)}\rangle$  and  $|\Phi_{(d)}\rangle$  because they have different flux-tube configurations. It is reasonable in the first order approximation, as mentioned before. In each tube configuration, the minimum length  $L_f$  is given by a sum of the lengths( $R_i$ ) of bonds  $L_f = R_1 + \dots + R_k$  ( $k$  is the number of the bonds. See Fig.2). Here we define  $L_{ij}$  to be the length of the path between  $i$ -th (anti)quark and  $j$ -th (anti)quark along the flux tubes. For example, in case of the  $[qq][qq]\bar{q}$  state shown in Fig.2(c), the path lengths are given by the bond lengths  $R_i$  as  $L_{12} = R_1 + R_2$ ,  $L_{13} = R_1 + R_6 + R_7 + R_3$ ,  $L_{1\bar{1}} = R_1 + R_6 + R_5$ , etc. Then we can rewrite  $L_f$  in the expectation values of the string potential  $\langle \Phi | H_f | \Phi \rangle$  with respect to a meson system( $\Phi_{q\bar{q}}$ ), a three-quark system( $\Phi_{q^3}$ ), and the pentaquark states  $\Phi_{(e)}$ ,  $\Phi_{(f)}$ ,  $\Phi_{(d)}$ , as follows:

$$L_f = L_{12} \quad \text{in } \langle \Phi_{q\bar{q}} | H_f | \Phi_{q\bar{q}} \rangle, \quad (4)$$

$$L_f = \frac{1}{2}(L_{12} + L_{23} + L_{31}) \quad \text{in } \langle \Phi_{q^3} | H_f | \Phi_{q^3} \rangle, \quad (5)$$

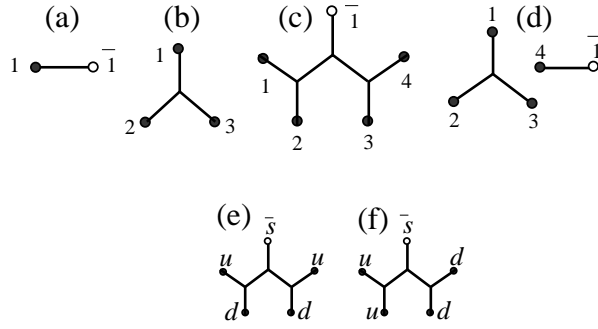


FIG. 1. Flux-tube configurations for confined states of  $q\bar{q}$  (a),  $q^3$  (b),  $q^4\bar{q}$  (c), and disconnected flux-tube of  $q^4\bar{q}$  (d). Figures (e) and (f) represent the flux tubes in the color configurations,  $[ud][ud]\bar{s}$  and  $[uu][dd]\bar{s}$ , respectively.

$$L_f = \frac{1}{2}(L_{12} + L_{34}) + \frac{1}{8}(L_{13} + L_{14} + L_{23} + L_{24}) + \frac{1}{4}(L_{\bar{1}1} + L_{\bar{1}2} + L_{\bar{1}3} + L_{\bar{1}4}) \quad \text{in } \langle \Phi_{(e,f)} | H_f | \Phi_{(e,f)} \rangle, \quad (6)$$

$$L_f = \frac{1}{2}(L_{12} + L_{23} + L_{31}) + L_{\bar{1}4} \quad \text{in } \langle \Phi_{(d)} | H_f | \Phi_{(d)} \rangle. \quad (7)$$

In the practical calculation, we approximate the minimum length of the flux tubes  $L_f$  by a linear combination of two-body distances  $r_{ij}$  between the  $i$ -th (anti)quark the  $j$ -th (anti)quark as,

$$L_f \approx r_{12} \quad \text{in } \langle \Phi_{q\bar{q}} | H_f | \Phi_{q\bar{q}} \rangle, \quad (8)$$

$$L_f \approx \frac{1}{2}(r_{12} + r_{23} + r_{31}) \quad \text{in } \langle \Phi_{q^3} | H_f | \Phi_{q^3} \rangle, \quad (9)$$

$$L_f \approx \frac{1}{2}(r_{12} + r_{34}) + \frac{1}{8}(r_{13} + r_{14} + r_{23} + r_{24}) + \frac{1}{4}(r_{\bar{1}1} + r_{\bar{1}2} + r_{\bar{1}3} + r_{\bar{1}4}) \quad \text{in } \langle \Phi_{(e,f)} | H_f | \Phi_{(e,f)} \rangle, \quad (10)$$

$$L_f \approx \frac{1}{2}(r_{12} + r_{23} + r_{31}) + r_{\bar{1}4} \quad \text{in } \langle \Phi_{(d)} | H_f | \Phi_{(d)} \rangle. \quad (11)$$

It is clear that the above equations are obtained by approximating the path length  $L_{ij}$  with the distance  $r_{ij}$  as  $L_{ij} \approx r_{ij}$  for all  $qq$  and  $q\bar{q}$  pairs. In the meson system, it is clear that Eq.8 gives the exact  $L_f$  value. The approximation, Eq.9, for  $3q$ -baryons is used in Ref. [24] and has been proved to be a good approximation. We note that the confinement is reasonably realized by the approximation in Eq.10 for  $\Phi_{(e,f)}$  as follows. The flux-tube configuration (e)(or (f)) consists of seven bonds and three junctions. In the limit that the length( $R_i$ ) of any  $i$ -th bond becomes much larger than other bonds, the string potential  $\langle H_f \rangle$  approximated by Eq.10 behaves as a linear potential  $\sigma R$ . It means that all the quarks and anti-quarks are bound by the linear potential with the tension  $\sigma$ . In that sense, the approximation in Eq.10 for the connected flux-tube configurations is regarded as a natural extension of the approximation(Eq.9) for  $3q$ -baryons. It is convenient to introduce an operator  $\mathcal{O} \equiv -\frac{3}{4}\sigma \sum_{i < j} F_i F_j r_{ij} - M^0$ . One can easily prove that the above approximations, 8,9,10,11, are equivalent to  $\langle \Phi | H_f | \Phi \rangle \approx \langle \Phi | \mathcal{O} | \Phi \rangle$  within each of the flux-tube configurations because the proper factors arise from  $F_i F_j$  depending on the color configurations of the corresponding  $qq$  (or  $q\bar{q}$ ) pairs.

In order to see the accuracy of the approximations Eqs.9 and 10, we calculate the ratio of the approximated length  $L_{app}$  to the exact  $L_f$  in a simple quark distribution with Gaussian form which imitates the model wave function of the present calculation. Figure 3 shows the ratio  $L_{app}/L_f$  in a  $q^3$  system and a  $[qq][qq]\bar{q}$  system. The quark positions  $\mathbf{r}_i$  are randomly chosen in Gaussian deviates with the probability  $\rho = \exp(-r_i^2/b^2)$ , and  $(L_f, L_{app}/L_f)$  values for 1000 samplings are plotted. We use the same size parameter  $b$  as that of the single-particle Gaussian wave function in the present model explained later. Comparing Figs.3(a) with 3(b), we found that the  $L_{app}/L_f$  ratio for the  $[qq][qq]\bar{q}$  system is about 10% smaller than that for the  $q^3$  system. Since the zero-point energy  $M_0$  in the string potential is adjusted in each of the  $q^3$  and the  $[qq][qq]\bar{q}$ , this underestimation should relate only to the relative energy of the string potential in each system, and may give a minor effect on the level structure of the pentaquark.

We solve the eigenstates of the Hamiltonian with a variational method in the AMD model space [22,23]. We take a base AMD wave function in a quark model as follows.

$$\Phi(\mathbf{Z}) = (1 \pm P) \mathcal{A} \left[ \phi_{\mathbf{Z}_1} \phi_{\mathbf{Z}_2} \cdots \phi_{\mathbf{Z}_{N_q}} X \right], \quad (12)$$

$$\phi_{\mathbf{Z}_i} = \left( \frac{1}{\pi b^2} \right)^{3/4} \exp \left[ -\frac{1}{2b^2} (\mathbf{r} - \sqrt{2} b \mathbf{Z}_i)^2 + \frac{1}{2} \mathbf{Z}_i^2 \right], \quad (13)$$

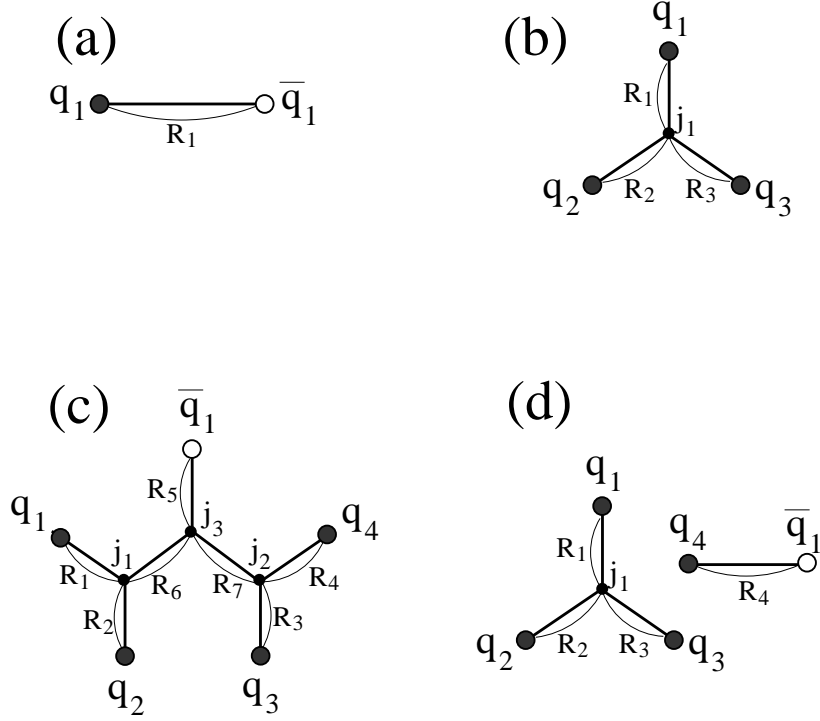


FIG. 2. Flux-tube topologies for the  $q\bar{q}$  (a),  $q^3$  (b),  $[q_1q_2][q_3q_4]\bar{q}_1$  (c), and disconnected flux tubes (d) for the  $(qqq)_1(q\bar{q})_1$ . The flux-tube topologies are described by the bonds with the lengths  $R_k$  and the junctions  $j_k$ .

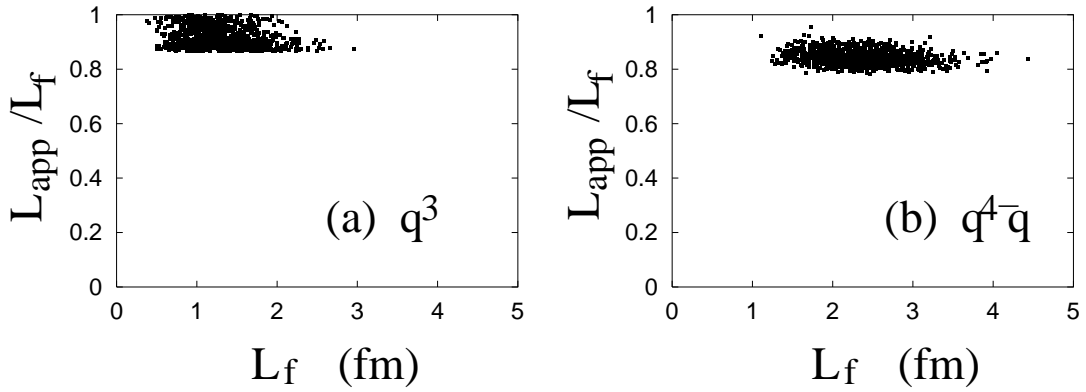


FIG. 3. The ratio  $L_{app}/L_f$  for the approximated tube length  $L_{app}$  and the exact tube length  $L_f$  in a  $q^3$  system and a  $[qq][qq]\bar{q}$  system. The quark positions  $\mathbf{r}_i$  are randomly chosen in Gaussian deviates with the probability  $\rho = \exp(-r_i^2/b^2)$ , and  $(L_f, L_{app}/L_f)$  values for 1000 samplings are plotted.

where  $1 \pm P$  is the parity projection operator,  $\mathcal{A}$  is the anti-symmetrization operator, and the spatial part  $\phi_{\mathbf{Z}_i}$  of the  $i$ -th single-particle wave function given by a Gaussian whose center is located at  $\mathbf{Z}_i$  in the phase space.  $X$  is the spin-isospin-color function. For example, in case of the proton,  $X$  is given as  $X = (|\uparrow\uparrow\uparrow\rangle_S - |\uparrow\uparrow\downarrow\rangle_S) \otimes |uud\rangle \otimes \epsilon_{abc}|abc\rangle_C$ . Here,  $|m\rangle_S (m = \uparrow, \downarrow)$  is the intrinsic-spin function and  $|a\rangle_C (a = 1, 2, 3)$  expresses the color function. Thus, the wave function of the  $N_q$  quark system is described by the complex variational parameters,  $\mathbf{Z} = \{\mathbf{Z}_1, \mathbf{Z}_2, \dots, \mathbf{Z}_{N_q}\}$ . By using the frictional cooling method [22] the energy variation is performed with respect to  $\mathbf{Z}$ .

For the pentaquark system ( $uudd\bar{s}$ ),

$$X = \sum_{m_1, m_2, m_3, m_4, m_5} c_{m_1 m_2 m_3 m_4 m_5} |m_1 m_2 m_3 m_4 m_5\rangle_S \otimes \{|udud\bar{s}\rangle \text{ or } |uudd\bar{s}\rangle\} \otimes \epsilon_{abg}\epsilon_{ceh}\epsilon_{ghf}|abce\bar{f}\rangle_C, \quad (14)$$

where  $|udud\bar{s}\rangle$  and  $|uudd\bar{s}\rangle$  correspond to the configurations  $[ud][ud]\bar{s}$  and  $[uu][dd]\bar{s}$  in Fig.1, respectively. Since we are interested in the confined states, we do not use the meson-baryon states,  $(qqq)_1(q\bar{q})_1$ . This assumption of decoupling of the reducible and irreducible configurations of the flux tubes can be regarded as a kind of bound-state approximation. The decoupling of the different flux-tube configurations can be characterized by the suppression factor  $\epsilon$  from the transition of the gluon field in the non-diagonal matrix elements  $\epsilon\langle\Phi_1|\mathcal{O}|\Phi_2\rangle$ . In a simple flux-tube model,  $\epsilon$  is roughly estimated by the area  $\Delta_s$  swept by the tubes when moving from one configuration into the other configuration as  $\epsilon \sim \exp(-\sigma\Delta_s)$ . We make an estimation of the expectation value of  $\exp(-\sigma\Delta_s)$  by assuming a simple quark distribution with Gaussian form which imitates the model wave function in the same way as the evaluation of the  $L_{app}/L_f$ . The suppression factor  $\epsilon$  among the configurations  $[ud][ud]\bar{s}$ ,  $[uu][dd]\bar{s}$ , and  $(qqq)_1(q\bar{q})_1$  is estimated to be  $\epsilon^2 \lesssim 1/10$  within the present model space. Therefore, we consider that the present assumption of the complete decoupling  $\epsilon = 0$  in the energy variation is acceptable in first order calculations.

The coefficients  $c_{m_1 m_2 m_3 m_4 m_5}$  for the spin function are determined by diagonalization of Hamiltonian and norm matrices. After the energy variation with respect to the  $\{\mathbf{Z}\}$  and  $c_{m_1 m_2 m_3 m_4 m_5}$ , the intrinsic-spin and parity  $S^\pi$  eigen wave function  $\Phi(\mathbf{Z})$  for the lowest state is obtained for each  $S^\pi$ . In the AMD wave function, the spatial wave function is given by multi-center Gaussians. When the Gaussian centers are located in some groups, the wave function describe the multi-center cluster structure and is equivalent to the Brink model wave function (a cluster model often used in nuclear structure study) [30,31]. On the other hand, because of the antisymmetrization, it can also represent shell-model wave functions when all the Gaussian centers are located near the center of the system [30,31]. In nuclear structure study, it has been already proved that the AMD is one of powerful tools due to the flexibility of the wave function [23]. In general, the relative motions in the AMD are given by such Gaussian forms as  $\exp[-\nu'(\mathbf{x} - \mathbf{R})^2]$  where  $\mathbf{x}$  is a Jacobi coordinate and  $\mathbf{R}$  is given by a linear combination of the Gaussian centers  $\{\mathbf{Z}_1, \mathbf{Z}_2, \dots, \mathbf{Z}_{N_q}\}$ . Here we explain the details of the relative motion in a simple case of a two-body cluster structure in a  $N_q = 5$  system. If the Gaussian centers are located in two groups as  $\mathbf{Z}_1 = \mathbf{Z}_2 = \mathbf{Z}_3 = \mathbf{Q}_1/\sqrt{2}b$  and  $\mathbf{Z}_4 = \mathbf{Z}_5 = \mathbf{Q}_2/\sqrt{2}b$ , and if each group does not contain identical particles, the wave function expresses the two-body cluster state, where each cluster is the harmonic oscillator 0s-orbital state,  $(0s)^{2,3}$ , with zero orbital-angular momentum. The inter-cluster motion  $\mathcal{X}$  is given as  $\mathcal{X}(\mathbf{x}, \mathbf{R}, \nu') = \exp[-\nu'(\mathbf{x} - \mathbf{R})^2]$ , where  $\nu' = \frac{3}{5b^2}$ ,  $\mathbf{R} = \mathbf{Q}_2 - \mathbf{Q}_1$  and  $\mathbf{x}$  is the relative coordinate between the clusters. In the partial wave expansion of the inter-cluster motion  $\mathcal{X}$ ,

$$\begin{aligned} \mathcal{X}(\mathbf{x}, \mathbf{R}, \nu') &= \exp[-\nu'(\mathbf{x} - \mathbf{R})^2], \\ &= \sum_L 4\pi i_L(2\nu'Rx)e^{-\nu'(x^2+R^2)} \sum_M Y_{LM}(\hat{x})Y_{LM}^*(\hat{R}), \end{aligned} \quad (15)$$

where  $i^L$  is the modified spherical Bessel function, it is found that the wave function contains higher orbital-angular momentum  $L$  components in general. However, in case of  $\nu'R^2 \leq O(1)$ , the wave function is dominated by the lowest  $L$  component since the  $L$  components rapidly decrease with the increase of  $L$ . As a result, the even-parity  $S^{\pi=+} 3^q$  and odd-parity  $q^4\bar{q}$  states are almost the  $L = 0$  eigen states, while the odd-parity  $3^q$  and even-parity  $q^4\bar{q}$  states are nearly the  $L = 1$  eigen states. (The  $q^4\bar{q}$  contains an odd intrinsic parity of the  $\bar{q}$  in addition to the parity of the spatial part.) Therefore, we do not perform the explicit  $L$ -projection in present calculation for simplicity. We have actually checked that the obtained wave functions are almost the  $L$ -eigen ( $L = 0$  or  $1$ ) states and higher  $L$  components are minor in most of the  $q^3$  and  $q^4\bar{q}$  states.

In the present wave function we do not explicitly perform the isospin projection, however, the wave functions obtained by energy variation are found to be approximately isospin-eigen states in most of the low-lying states of the  $q^3$  and  $q^4\bar{q}$  due to the color-spin symmetry.

In the numerical calculation, the linear and Coulomb potentials are approximated by seven-range Gaussians. We use the following parameters,

$$\begin{aligned} \alpha_c &= 1.05, \\ \Lambda &= 0.13 \text{ fm}, \end{aligned}$$

TABLE I. Calculated masses (GeV) of the  $q^3$  systems. The expectation values of the kinetic, string, Coulomb and color-magnetic terms are also listed.

$S^\pi$	$(uud)_1$ $\frac{1}{2}^+$	$(uud)_1$ $\frac{1}{2}^-$	$(uuu)_1$ $\frac{3}{2}^+$	$(uds)_1$ $\frac{1}{2}^+$	$(uds)_1$ $\frac{1}{2}^-$
Kinetic( $H_0$ )	1.74	1.87	1.66	1.93	2.09
String( $H_F$ )	0.02	0.27	0.07	0.03	0.25
Coulomb	-0.65	-0.52	-0.62	-0.65	-0.53
Color mag.	-0.17	-0.09	0.14	-0.16	-0.14
$E$	0.94	1.52	1.24	1.14	1.67
exp. (MeV)	$N(939)$	$N^*(1520), N^*(1535)$	$\Delta(1232)$	$\Lambda(1115)$	$\Lambda(1670)$

TABLE II. Calculated masses(GeV) of the  $uudd\bar{s}$  system.  $M_{q^4\bar{q}}^0=2385$  MeV is used to adjust the energy of the lowest state to the observed mass. The expectation values of the kinetic, string, Coulomb, color-magnetic terms, and that of the color-magnetic term in  $q\bar{q}$  pairs are listed. In addition to the lowest  $1/2^-$  state with the  $[uu][dd]\bar{s}$  configuration, we also show the results of the  $1/2^-$  state with  $[ud][ud]\bar{s}$  configuration, which lies in the low-energy region.

$S^\pi$	$[uu][dd]\bar{s}$ $\frac{1}{2}^-$	$[ud][ud]\bar{s}$ $\frac{3}{2}^-$	$[ud][ud]\bar{s}$ $\frac{1}{2}^+$	$[ud][ud]\bar{s}$ $\frac{1}{2}^-$	$[uu][dd]\bar{s}$ $\frac{5}{2}^-$	$[ud][ud]\bar{s}$ $\frac{3}{2}^+$	$[ud][ud]\bar{s}$ $\frac{5}{2}^+$
Kinetic( $H_0$ )	3.23	3.22	3.36	3.19	3.19	3.36	3.33
String( $H_F$ )	-0.67	-0.66	-0.55	-0.64	-0.64	-0.56	-0.54
Coulomb	-1.05	-1.04	-0.99	-1.03	-1.03	-0.99	-0.98
Color mag.	-0.01	0.01	-0.25	0.04	0.19	-0.06	0.17
$q\bar{q}$ Color mag.	-0.06	-0.01	0.00	0.02	0.06	0.02	0.04
$E$	1.50	1.53	1.56	1.56	1.71	1.75	1.98

$$\begin{aligned}
m_q &= 0.313 \text{ GeV}, \\
m_s &= 0.513 \text{ GeV}, \\
\sigma &= 0.853 \text{ GeV/fm}.
\end{aligned} \tag{16}$$

Here, the quark-gluon coupling constant  $\alpha_c$  is chosen so as to fit the  $N$  and  $\Delta$  mass difference. The string tension  $\sigma$  is adopted to adjust the excitation energy of  $N^*(1520)$ . The size parameter  $b$  is chosen to be 0.5 fm.

### III. RESULTS

In table.I, we display the calculated energy of  $q^3$  states with  $S^\pi = 1/2^+(N)$ ,  $S^\pi = 3/2^+(\Delta)$ ,  $S^\pi = 1/2^-(N^*)$ . The zero-point energy  $M^0$  of the string potential is chosen to be  $M_{q^3}^0 = 972$  MeV to fit the masses of  $q^3$  systems,  $N$ ,  $N^*$  and  $\Delta$ . The calculated masses for  $\Lambda$  with  $S^\pi = 1/2^-$  and  $1/2^+$  correspond to the experimental data of  $\Lambda(1115)$  and  $\Lambda^*(1670)$ . The contributions of the kinetic and each potential terms are consistent with the results of the Ref. [26]. We checked that the obtained states are almost eigen states of the angular momentum  $L$  and the  $L$  projection gives only minor effects on the energy.

Now, we apply the AMD method to the  $uudd\bar{s}$  system. For each spin parity, we calculate energies of the  $[ud][ud]\bar{s}$  and  $[uu][dd]\bar{s}$  states and adopt the lower one. In table.II, the calculated results are shown. We adjust the zero-point energy of the string potential  $M_0$  as  $M_{q^4\bar{q}}^0 = 2385$  MeV to fit the absolute mass of the recently observed  $\Theta^+$ . This  $M_{q^4\bar{q}}^0$  for pentaquark system is chosen independently of  $M_{q^3}^0$  for  $3q$ -baryon. If  $M_{q^4\bar{q}}^0 = \frac{5}{3}M_{q^3}^0$  is assumed as Ref. [26], the calculated mass of the pentaquark is around 2.2 GeV, which is consistent with the result of Ref. [26].

The most striking point in the results is that the  $S^\pi = 3/2^-$  and  $S^\pi = 1/2^+$  states nearly degenerate with the  $S^\pi = 1/2^-$  states. The  $S^\pi = 1/2^+$  correspond to  $J^\pi = \{1/2^+, 3/2^+\}$  ( $S = 1/2, L = 1$ ), and the  $S^\pi = 3/2^-$  is  $J^\pi = 3/2^-$  ( $S = 3/2, L = 0$ ). The lowest  $S^\pi = 1/2^-$  ( $J^\pi = 1/2^-, L = 0$ ) state appears just below the  $S^\pi = 3/2^-$  and the second  $S^\pi = 1/2^-$  ( $J^\pi = 1/2^-, L = 0$ ) state is at the same energy as the  $S^\pi = 1/2^+$  ( $J^\pi = 1/2^+, 3/2^+, L = 1$ ) states. However these  $J^\pi = 1/2^-$  states, as we discuss later, are expected to be much broader than other states. The  $J^\pi = 1/2^+$  and  $3/2^+$  exactly degenerate in the present Hamiltonian which does not contain the spin-orbit force. Other spin-parity states are much higher than these low-lying states.

## IV. DISCUSSION

In this section, we analyze the structure of the obtained low-lying states of the  $uudd\bar{s}$  system, and discuss the level structure and the width for  $KN$  decays.

### A. Structure of low-lying states

We analyze the spin structure of these states, and found that the  $J^\pi = \{1/2^+, 3/2^+\}$  states consist of two spin-zero  $[ud]$ -pairs, while the  $J^\pi = 3/2^-$  contains of a spin-zero  $[ud]$ -pair and a spin-one  $[ud]$ -pair. Here we call the color anti-triplet  $qq$  pair with the same spatial single-particle wave functions as a  $[qq]$ -pair and note a spin  $S$   $[qq]$ -pair as  $[qq]^S$ . Since the  $[ud]^0$ -pair has the isospin  $I = 0$  and the  $[ud]^1$ -pair has the isospin  $I = 1$  because of the color asymmetry, the  $J^\pi = 3/2^-$  state is isovector while the lowest even-parity  $J^\pi = \{1/2^+, 3/2^+\}$  states are isoscalar. The  $J^\pi = 1/2^+$  state corresponds to the  $\Theta^+(1530)$  in the flavor  $\overline{10}$ -plet predicted by Diakonov et al. [13]. It is surprising that the odd-parity state,  $J^\pi = 3/2^-$  has the isospin  $I = 1$ , which means that this state is a member of the flavor 27-plet and belong to a new family of  $\Theta$  baryon. We denote the  $J^\pi = \{1/2^+, 3/2^+\}$ ,  $I = 0$  states by  $\Theta_0^+$ , and the  $J^\pi = 3/2^-$ ,  $I = 1$  state by  $\Theta_1^+$ . The mass difference  $E(\Theta_0^+) - E(\Theta_1^+)$  is about 30 MeV. In the energy region compatible to the  $J^\pi = \{1/2^+, 3/2^+\}$  and  $J^\pi = 3/2^-$  states, there appear two  $J^\pi = \{1/2^-\}$  states. The lowest one is the  $[uu][d\bar{d}]\bar{s}$  state with  $[uu]^1$  and  $[d\bar{d}]^1$  pairs, while the higher one is the  $[ud][u\bar{d}]\bar{s}$  with  $[ud]^0$  and  $[u\bar{d}]^1$  pairs. The former is the isospin symmetric state and is dominated by  $I = 0$  component. The latter is isovector and is regarded as the spin  $S$ -partner of the  $J^\pi = 3/2^-$  state. The  $J^\pi = 1/2^-$  state is the lowest in the  $uudd\bar{s}$  system. We, however, consider this state not to be the observed  $\Theta^+$  because its width should be broad as discussed later.

Although it is naively expected that unnatural spin parity states are much higher than the natural spin-parity  $1/2^-$  state, the present results show the abnormal level structure of the  $(uud\bar{s})$  system, where the high spin  $J^\pi = 3/2^-$  state and the unnatural parity  $J^\pi = \{1/2^+, 3/2^+\}$  states nearly degenerate just above the  $J^\pi = 1/2^-$  state. By analysing the details of these states, the abnormal level structure can be easily understood with a simple picture as follows. As shown in table II, the  $J^\pi = \{1/2^+, 3/2^+\}$  ( $L = 1$ ) states have larger kinetic and string energies than the  $J^\pi = 3/2^-$  ( $L = 0$ ) and  $J^\pi = 1/2^-$  ( $L = 0$ ) states, while the former states gain the color-magnetic interaction. It indicates that the degeneracy of parity-odd states and parity-even states is realized by the balance of the loss of the kinetic and string energies and the gain of the color-magnetic interaction. In the  $J^\pi = \{1/2^+, 3/2^+\}$  and the  $J^\pi = 1/2^-, 3/2^-$  states, the competition of the energy loss and gain can be understood by Pauli principle from the point of view of the  $[qq]$ -pair structure as follows. As already mentioned by Jaffe and Wilczek [14], the relative motion between two  $[qq]^0$ -pairs must have the odd parity ( $L = 1$ ) because the  $L = 0$  is forbidden between the two identical  $[qq]$ -pairs due to the color antisymmetry. In the  $J^\pi = 3/2^-$  state and the second  $J^\pi = 1/2^-$  state, one of  $[ud]^0$ -pairs is broken to be a  $[ud]^1$ -pair and the  $L = 0$  is allowed because two diquarks are not identical. The  $L = 0$  is energetically favored in the kinetic and string terms, and the energy gain cancels the color-magnetic energy loss of a  $[ud]^1$ -pair. Also in the lowest  $J^\pi = 1/2^-$  state, the competition of energy loss and gain is similar as each contribution of the kinetic, string and potential energies in the lowest  $J^\pi = 1/2^-$  state is almost the same as those in the  $J^\pi = 3/2^-$  and the second  $J^\pi = 1/2^-$  (table II). It means that the gain of the kinetic energy of the  $L = 0$  state compete with the color-magnetic energy loss in the lowest  $J^\pi = 1/2^-$  as well as the  $J^\pi = 3/2^-$  and the second  $J^\pi = 1/2^-$ .

We should stress that the existence of two spin-zero  $ud$ -diquarks in the  $J^\pi = \{1/2^+, 3/2^+\}$  states predicted by Jaffe and Wilczek [14] is actually confirmed in the present calculations without *a priori* assumptions for the spin and spatial configurations. In fact, the component with two spin-zero  $[ud]$ -pairs is 97% in the present  $J^\pi = \{1/2^+, 3/2^+\}$  state. In Fig. 4, we show the quark and anti-quark density distribution in the  $J^\pi = \{1/2^+, 3/2^+\}$  states and display the centers of Gaussians for the single-particle wave functions. In the intrinsic wave function, Gaussian centers for two  $[ud]^0$ -pairs are located far from each other with the distance about 0.6 fm. It indicates the spatially developed diquark-cluster structure, which means the spatial and spin correlations in each  $[ud]$ -pair. It is found that the center of the  $\bar{s}$  stays at the same point of that of one  $[ud]^0$ , as  $\mathbf{Z}_1 = \mathbf{Z}_2 = \frac{3}{5\sqrt{2}b}\mathbf{Q}_{12}$  and  $\mathbf{Z}_3 = \mathbf{Z}_4 = \mathbf{Z}_5 = -\frac{2}{5\sqrt{2}b}\mathbf{Q}_{12}$  where  $\{\mathbf{Z}_1, \mathbf{Z}_2, \dots, \mathbf{Z}_5\}$  are the Gaussian centers in Eq. 12 and  $|\mathbf{Q}_{12}| \sim 0.6$  fm. As a result, we found the spatial development of  $ud$ - $uds$  clustering and a parity-asymmetric shape in the intrinsic state before parity projection (Fig. 4). As explained in II, the wave function is equivalent to the  $[ud]^0$ - $[ud]^0\bar{s}$  cluster wave function in Brink model [30] with  $L = 1$  relative motion. After the parity projection, the  $\bar{s}$  is exchanged between two diquarks. In contrast to the spatially developed cluster structure in the even-parity state, the odd-parity states  $J^\pi = 1/2^-, 3/2^-$  are almost the spatially symmetric  $(0s)^5$  states with spherical shapes.

As mentioned before, the degeneracy of the even-parity states and the odd-parity states originates in the balance of the  $L = 1$  excitation energy and the energy gain of the color-magnetic interaction. Here we consider the  $L = 1$  excitation energy  $\Delta E(L = 1)$  as the total energy loss in the kinetic, string and Coulomb terms. It is important that

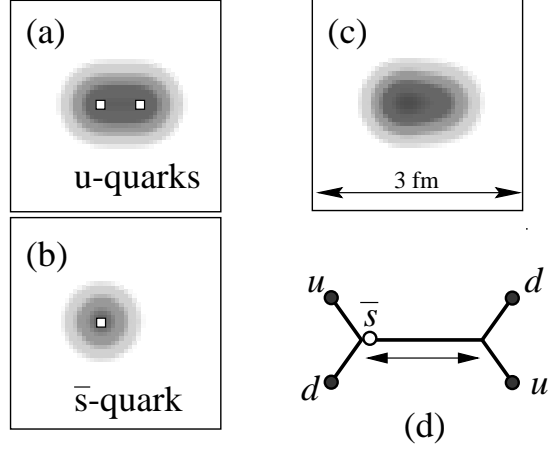


FIG. 4. The  $q$  and  $\bar{q}$  density distribution in the  $J^\pi = 1/2^+, 3/2^+ (S = 1/2, L = 1)$  states of the  $uudd\bar{s}$  system. The  $u$  density (a),  $\bar{s}$  density (b), and total quark-antiquark density (c) of the intrinsic state before parity projection are shown. The schematic figure of the corresponding flux-tube configuration is illustrated in (d). Open squares in (a) and (b), indicate the positions of Gaussian centers  $\text{Re}[\sqrt{2}b\mathbf{Z}_i]$  for the  $i$ -th single-particle wave functions.

$\Delta E(L = 1) \sim 0.3$  GeV in the pentaquark is much smaller than  $\Delta E(L = 1) \sim 0.5$  GeV in the nucleon system. The reason for the relatively small  $\Delta E(L = 1)$  in the pentaquark can be easily understood by the  $ud$ - $uds$  cluster structure. In the two-body cluster state with the  $L = 1$  relative motion, the  $\Delta E(L = 1)$  is roughly estimated by the reduced mass  $\mu = A_1 A_2 / (A_1 + A_2)$  of two clusters, as is given as  $\Delta E(L = 1) \propto \frac{1}{\mu}$  ( $A_1$  and  $A_2$  are the masses of the clusters). In the nucleon,  $\mu = \frac{2}{3}m_q$  is obtained from the  $ud$ - $u$  cluster structure in the  $J^\pi = 1/2^- (L = 1)$  state, while  $\mu \sim \frac{6}{5}m_q$  for the pentaquark system is found in the  $ud$ - $uds$  clustering. The reduced mass in the pentaquark is  $9/5$  times larger than that in the nucleon system, therefore,  $\Delta E(L = 1)$  should be smaller in the pentaquark than in the nucleon by the factor  $5/9$ . This factor is consistent with the present  $\Delta E(L = 1)$  values.

We give a comment on the  $LS$ -splitting between  $J^\pi = 1/2^+$  and  $3/2^+ (S = 1/2, L = 1)$ . In the present calculation, where the spin-orbit force is omitted, the  $J^\pi = 1/2^+$  and  $3/2^+$  states exactly degenerate. Even if we introduce the spin-orbit force into the Hamiltonian, the  $LS$ -splitting should not be large in this diquark structure because the effect of the spin-orbit force from the spin-zero diquarks is very weak as discussed in Ref. [33].

We remark that the  $[ud]^0$ - $[ud]^0\bar{s}$  cluster structure in the present result is different from the diquark-triquark structure proposed by Karliner and Lipkin [16] because the  $ud\bar{s}$ -triquark in Ref. [16] is the  $(us)_6^{S=1}\bar{s}$  with the color-symmetric spin-one  $ud$ -diquark. In the  $(us)_6^{S=1}\bar{s}$ -triquark, the  $\bar{s}$  quark should be tightly bound in the triquark due to the strong color-magnetic interaction between  $(us)_6^{S=1}$  and  $\bar{s}$ . On the other hand, in the present  $[ud]^0\bar{s}$ -cluster, the  $\bar{s}$  feels no strong color-magnetic interaction and is bound more weakly than in the  $(us)_6^{S=1}\bar{s}$ -triquark. The color-6 flux tubes are not taken into account in the present framework since they are excited. However, the  $(us)_6^{S=1}\bar{s}$ -triquark might be possible if the short-range correlation in the triquark make the flux-tube short enough to be excited into the color-6 flux-tube.

## B. Width for $KN$ decays

In the  $\Theta^+ \rightarrow KN$  decays, it is important that the allowed decay mode in the  $\Theta_1^+ (J^\pi = 3/2^-)$  is  $D$  wave, which should make the  $\Theta_1^+$  state narrower than the  $\Theta_0^+ (J^\pi = 1/2^+, 3/2^+)$  because of higher centrifugal barrier. We estimate the  $KN$ -decay widths of these states by using a method of reduced width amplitudes [31,32]. This method has been applied for the study of  $\alpha$ -decay width in the nuclear physics within bound state approximations. In this method, the decay width  $\Gamma$  is estimated by the penetrability  $P_L(k, a)$  of the barrier and the reduced width  $\gamma^2(a)$  as a function of the threshold energy  $E_{th}$  and the channel radius  $a$ ,

$$\Gamma = 2P_L(k, a)\gamma^2(a),$$

$$P_L(k, a) = \frac{ka}{j_L^2(ka) + n_L^2(ka)},$$



$$\gamma^2(a) = \frac{\hbar^2}{2\mu a} S_{fac}(a), \quad (17)$$

where  $\mu$  is the reduced mass,  $k$  is the wave number  $k = \sqrt{2\mu E_{th}/\hbar^2}$ , and  $j_L(n_L)$  is the regular(irregular) spherical Bessel function.  $S_{fac}(a)$  is the probability of decaying particle at the channel radius  $a$ . We define  $\Gamma_L^0(a, E_{th}) \equiv \frac{\hbar^2 k}{\mu} \frac{1}{j_L^2(ka) + n_L^2(ka)}$ , then, the decay width can be rewritten in a simple form as  $\Gamma = \Gamma_L^0 \times S_{fac}$ . In the following discussion, we choose the channel radius  $a = 1$  fm and  $E_{th} = 100$  MeV. Since the transitions between the different flux-tube configurations, a confined state  $[ud][ud]\bar{s}$  and a decaying state  $(udd)_1(u\bar{s})_1$ , are of higher order, the  $S_{fac}$  should be small in general when the suppression by the flux-tube transition is taken into account. Here, we evaluate the maximum values of the widths for the  $J^\pi = 1/2^+, 3/2^+$  states with the method of the reduced width amplitudes, by using meson-baryon probability considering only the simple overlap for the quark wave functions.

In case of even-parity  $J^\pi = 1/2^+, 3/2^+$  states, the  $KN$  decay modes are the  $P$ -wave, which gives  $\Gamma_{L=1}^0 \approx 100$  MeV fm. By assuming  $(0s)^2$  and  $(0s)^3$  harmonic-oscillator wave functions for  $K^0$  and  $p$ , we calculate the overlap between the obtained pentaquark wave function and the  $K^0 p$  state. As explained in the previous subsection, the  $J^\pi = 1/2^+, 3/2^+$  states have the  $ud$ - $ud\bar{s}$  cluster structure where five Gaussian centers are written as  $\mathbf{Z}_1 = \mathbf{Z}_2 = \frac{3}{5\sqrt{2}b}\mathbf{Q}_{12}$  and  $\mathbf{Z}_3 = \mathbf{Z}_4 = \mathbf{Z}_5 = -\frac{2}{5\sqrt{2}b}\mathbf{Q}_{12}$ . We assume a simple  $K^0 p$  wave function as follows,

$$\Phi_{K^0 p} = (1 + P)\mathcal{A} \left[ \phi_{\mathbf{Z}_1} \phi_{\mathbf{Z}_2} \cdots \phi_{\mathbf{Z}_{N_q}} X \right], \quad (18)$$

$$\phi_{\mathbf{Z}_i} = \left( \frac{1}{\pi b^2} \right)^{3/4} \exp \left[ -\frac{1}{2b^2} (\mathbf{r} - \sqrt{2}b\mathbf{Z}_i)^2 + \frac{1}{2}\mathbf{Z}_i^2 \right], \quad (19)$$

where the  $\mathbf{Z}_a$  are chosen as  $\mathbf{Z}_1 = \mathbf{Z}_2 = \mathbf{Z}_3 = a\frac{2}{5\sqrt{2}b}\mathbf{Q}_{12}/|\mathbf{Q}_{12}|$ ,  $\mathbf{Z}_4 = \mathbf{Z}_5 = -a\frac{3}{5\sqrt{2}b}\mathbf{Q}_{12}/|\mathbf{Q}_{12}|$ , and the spin-isospin-color wave function is taken to be

$$X = \sum_{m_1, m_2, m_3, m_4, m_5} c_{m_1 m_2 m_3 m_4 m_5} |m_1 m_2 m_3 m_4 m_5\rangle_S \otimes |udud\bar{s}\rangle \otimes \epsilon_{abc} \delta_{ef} |abce\bar{f}\rangle_C. \quad (20)$$

The same size parameter  $b$  as that of the pentaquark is used. The coefficients  $c_{m_1 m_2 m_3 m_4 m_5}$  for the spin function are taken to express the  $J^\pi = 1/2^+$  proton and the pseudoscalar  $K^0$  meson. The probability  $S_{fac}$  is evaluated by the overlap with the obtained  $J^\pi = 1/2^+, 3/2^+$  wave function,  $S_{fac} = |\langle \Phi_{K^0 p} | \Phi(\mathbf{Z}) \rangle|^2$ . (The  $\Phi_{K^0 p}$  and  $\Phi(\mathbf{Z})$  are normalized.) The probability  $S_{fac} = 0.034$  fm $^{-1}$  is evaluated by the overlap. Roughly speaking, the main factors in this meson-baryon probability are the factor  $\frac{1}{3}$  from the color configuration, the factor  $\frac{1}{4}$  from the intrinsic spin part, and the other factor which arises from the spatial overlap. By using the probability  $S_{fac} = 0.034$ , the  $K^0 p$  partial decay width is evaluated as  $\Gamma < 3.4$  MeV. The  $K^+ n$  decay width is the same as that of the  $K^0 p$  decay, and the total width of the  $J^\pi = 1/2^+, 3/2^+$  states is estimated to be  $\Gamma < 7$  MeV. This is consistent with the discussion in Ref. [34].

It is interesting that the  $KN$  decay width of the  $\Theta_1^+(J^\pi = 3/2^-)$  is strongly suppressed by the  $D$ -wave centrifugal barrier, because lower spin ( $S$ -wave and  $P$ -wave) decays are forbidden due to the conservation of spin and parity. Consequently,  $\Gamma_{L=2}^0$  is  $\approx 30$  MeV fm, which is much smaller than that for the  $P$ -wave case. Moreover, the  $\Theta_1^+(J^\pi = 3/2^-)$  is the state with  $S^\pi = 3/2^-$  and  $L = 0$ , which has no overlap with the  $KN(S^\pi = 1/2^-$  and  $L = 2)$  states in the present calculation because the spin-orbit or tensor forces are omitted. If we introduce the spin-orbit or tensor forces, the  $D$ -state( $S^\pi = 1/2^-$  and  $L = 2$ ) will be slightly mixed into the  $\Theta_1^+(J^\pi = 3/2^-)$ . However, the mixing component should be small because of the dominant central force in the potential. In other words, the  $KN$  probability( $S_{fac}$ ) in the  $\Theta_1^+(J^\pi = 3/2^-)$  state is expected to be rather suppressed than that in the  $\Theta_0^+(J^\pi = 1/2^+, 3/2^+)$  states. Considering the suppression effects in both terms  $\Gamma^0$  and  $S_{fac}$ , the  $J^\pi = 3/2^-$  state should be extremely narrow. If we assume the  $S_{fac}$  in the  $J^\pi = 3/2^-$  to be half of that in the  $J^\pi = 1/2^+, 3/2^+$  states, the  $KN$  decay width is estimated to be  $\Gamma < 1$  MeV.

Contrary to the narrow width of the  $J^\pi = 3/2^-$  state, the  $J^\pi = 1/2^-$  state should be much broader than other states because  $S$ -wave( $L = 0$ ) decay is allowed and therefore the centrifugal barrier is absent. We cannot evaluate the width of the  $J^\pi = 1/2^-$  states with the present method, since the method of the reduced width amplitudes works only when there exist barriers in the decaying channels. If we adopt the theoretical width  $\Gamma = 1.1$  GeV for the  $J^\pi = 1/2^-$  states in [34] and the suppression factor  $\epsilon^2 \lesssim 1/10$  due to the string transition, the width is evaluated to be  $\Gamma \sim 100$  MeV, which is still too large to describe that of the observed  $\Theta^+$ . We consider that the  $J^\pi = 1/2^-$  states may melt away due to the coupling with  $KN$  continuum states with no centrifugal barrier.

Also in other spin-parity states, the coupling with the  $KN$  continuum states is important for more quantitative discussions on the widths. We should point out that, in introducing the meson-baryon coupling, one should not treat only the quark degrees of freedom but take into account the suppression due to the rearrangement of flux-tube topologies between the meson-baryon states and the confined states.

## V. SUMMARY

We proposed a quark model in the framework of the AMD method, and applied it to the  $uudd\bar{s}$  system. The level structure of the  $uudd\bar{s}$  system and the properties of the low-lying states were studied within the model space of the  $[qq][q\bar{q}]\bar{q}$  configuration, where all the (anti)quarks are connected by the color-3 flux tubes. We predicted that the narrow  $J^\pi = \{1/2^+, 3/2^+\}(\Theta_0)$  and  $J^\pi = 3/2^- (\Theta_1)$  states nearly degenerate with the  $J^\pi = 1/2^-$  states. The widths of the  $J^\pi = \{1/2^+, 3/2^+\}$  states and the  $3/2^-$  state are estimated to be  $\Gamma < 7$  MeV and  $\Gamma < 1$  MeV, respectively. On the other hand, the  $J^\pi = 1/2^-$  states should be broad, and we consider that they may melt away due to the coupling with  $KN$  continuum states with no centrifugal barrier. Two spin-zero diquarks are found in the  $\{1/2^+, 3/2^+\}$  states, which confirms Jaffe-Wilczek picture. We comment that the formation of two spin-zero diquarks does not always occur in  $J^\pi = \{1/2^+, 3/2^+\}$  pentaquarks. For example, in case of the  $ddss\bar{u}$  system, the diquark structure disappears. Instead, a  $dss\bar{d}\bar{u}$  clustering appears in the  $J^\pi = \{1/2^+, 3/2^+\}$   $[ds][ds]\bar{u}$  states because the color magnetic interaction is weaker for  $ds$  pairs than for  $d\bar{u}$  pairs in OGE potential. In other words, the diquark structure is formed in such a certain pentaquark as the  $\Theta_0^+$  due to the strong color-magnetic attraction between  $ud$  quarks. The degeneracy of the  $J^\pi = 1/2^-, 3/2^-, 1/2^+$  and  $3/2^+$  states is realized by the balance of the kinetic and string energies and the color-magnetic interaction. The origin of the novel level structure is due to the color structure in the confined five quark system bound by the connected flux-tubes.

The  $J^\pi = \{1/2^+, 3/2^+\}(\Theta_{I=0}^+)$  states in the present results may be assigned to the experimentally observed  $\Theta^+$ , while  $J^\pi = 3/2^- (\Theta_{I=1})$  is not observed yet. One should pay attention to the properties of these states, because the production rates depend on their spin, parity and widths. The existence of many narrow states,  $J^\pi = 1/2^+, 3/2^+$ , and  $3/2^-$ , for the  $\Theta_0^+$  and  $\Theta_1^+$  may help to explain the inconsistent mass positions of the  $\Theta^+$  among the different experiments. Especially, the double peaks of the  $J^\pi = 1/2^+$  and  $3/2^+$  states in the  $\Theta_0^+$  are expected. In the  $\Theta_0^+$  peaks observed in the invariant mass or missing mass spectra, it is difficult to find the possible double peaks because the statistics and the resolutions are not enough [1–9]. The analysis of the  $NK$  scattering [35] provided the upper limit  $\Gamma < 1$  MeV for the widths of each peaks. Considering the suppression factor due to the gluon transitions, the possibility of the double peaks ( $J^\pi = 1/2^+$  and  $3/2^+$ ) suggested in the present works has not been excluded yet. We should comment that another explanation for the inconsistency of the experimental mass positions was suggested in Ref. [36], where a systematic lowering in mass of  $K^0p$  peaks relative to the  $K^+n$  was noted. In the  $I = 1$  channel, there is no significant  $\Theta^{++}$  signal in the experimental data of the invariant  $K^+p$  mass in the photo-induced reactions [5,9,37]. It is important that the widths of the  $J^\pi = 3/2^- \Theta_{I=1}$  should be about one order smaller than those of the  $J^\pi = 1/2^+$  and  $3/2^+$  for the  $\Theta_0^+$ . For the  $\Theta^{++}$  search, it would be helpful to choose proper entrance and decay channels based on the further investigation of the production mechanism. In order to compare the present findings with the experimental data in more details, further experimental data with high resolution and high statistics are required.

Finally, we would like to remind the readers that the absolute masses of the pentaquark in the present work are not predictions. We have an ambiguity of the zero-point energy of the string potential, which depends on the flux-tube topology in each of meson, three-quark baryon, pentaquark systems. In the present calculation of the pentaquark, we phenomenologically adjust it to reproduce the observed mass of the  $\Theta^+$ . In order to predict absolute masses of unknown multiquarks with new flux-tube topologies, it is desirable to determine the zero-point energy more theoretically.

The authors would like to thank to T. Kunihiro, Y. Akaishi and H. En'yo for valuable discussions. This work was supported by Japan Society for the Promotion of Science and Grants-in-Aid for Scientific Research of the Japan Ministry of Education, Science Sports, Culture, and Technology.

- 
- [1] LEPS collaboration, T. Nakano *et al.*, Phys. Rev. Lett. **91** (2003) 012002.
  - [2] DIANA Collaboration, V. V. Barmin *et al.*, Phys. Atom. Nucl. **66** (2003) 1715.
  - [3] CLAS Collaboration, S. Stepanyan *et al.*, Phys. Rev. Lett. **91** (2003) 252001.
  - [4] CLAS Collaboration, V. Kubarovsky *et al.*, Phys. Rev. Lett. **92** (2004) 032001
  - [5] SAPHIR Collaboration, J. Barth *et al.*, Phys. Lett. **B572** (2003) 127
  - [6] A. E. Asratyan, A. G. Dolgolenko and M. A. Kubantsev, [hep-ex/0309042](#).
  - [7] HERMES Collaboration, A. Airapetian *et al.*, [hep-ex/0312044](#).
  - [8] SVD Collaboration, A. Aleev *et al.*, [hep-ex/0401024](#).
  - [9] ZEUS Collaboration, S. V. Chekanov, [hep-ex/0404007](#).

- [10] BES Collaboration, J.Z. Bai *et al.*, [hep-ex/0402012](#).
- [11] HERA-B Collaboration, K.T. Knöpfle *et al.*, [hep-ex/0403020](#).
- [12] PHENIX Collaboration, C. Pinkenburg *et al.*, [nucl-ex/0404001](#).
- [13] D. Diakonov, V. Petrov and M. V. Polyakov, *Z. Phys.* **A359** (1997) 305.
- [14] R. Jaffe and F. Wilczek, *Phys. Rev. Lett.* **91** (2003) 232003.
- [15] S. Capstick, P. R. Page and W. Roberts, *Phys. Lett.* **B570** (2003) 185.
- [16] M. Karliner and H. J. Lipkin, *Phys. Lett.* **B575** (2003) 249.
- [17] A. Hosaka, *Phys. Lett.* **B571** (2003) 55.
- [18] J. Sugiyama, T. Doi and M. Oka, *Phys. Lett.* **B581** (2004) 167.
- [19] S. Sasaki, [hep-lat/0310014](#).
- [20] F. Csikor, Z. Fodor, S. D. Katz and T. G. Kovacs, *JHEP* **0311** 070 (2003).
- [21] B. K. Jennings and K. Maltman, *Phys. Rev.* **D69** (2004) 094020.
- [22] Y. Kanada-En'yo, H. Horiuchi and A. Ono, *Phys. Rev. C* **52** (1995) 628 ; Y. Kanada-En'yo and H. Horiuchi, *Phys. Rev. C* **52** (1995) 647 .
- [23] Y. Kanada-En'yo, M. Kimura and H. Horiuchi, *Comptes Rendus Physique* Vol.4 (2003) 497.
- [24] J. Carlson, J.B. Kogut and V. R. Pandharipande, *Phys. Rev.* **D27** (1983) 233; *Phys. Rev.* **D28** (1983) 2807.
- [25] O. Morimatsu, *Nucl. Phys.* **A505** (1989) 655; C. Alexandrou, T. Karapiperis and O. Morimatsu, *Nucl. Phys.* **A518** (1990) 723.
- [26] J. Carlson and V. R. Pandharipande, *Phys. Rev.* **D43** (1991) 1652.
- [27] T. T. Takahashi, H. Matsufuru, Y. Nemoto and H. Suganuma, *Phys. Rev. Lett.* **86** (2001) 18-21; T. T. Takahashi, H. Suganuma, Y. Nemoto and H. Matsufuru, *Phys. Rev.* **D65** (2002) 114509.
- [28] J. Kogut and L. Susskind, *Phys. Rev.* **D11** (1975) 395.
- [29] F. Okiharu, H. Suganuma, and T. T. Takahashi, [hep-lat/0407001](#).
- [30] D. Brink, *Proc. Int. School of Phys.* "ENRICO FERMI", course 36, p. 247.
- [31] H. Horiuchi and K. Ikeda, *Cluster Model of the Nucleus, International Review of Nuclear Physics*, ed. T. T. S. Kuo and E. Osnes (World Scientific, Singapore, 1985), vol. 4, pp.1.
- [32] H. Horiuchi and Y. Suzuki, *Prog. Theor. Phys.* **49** (1973) 1974, and references therein.
- [33] By J.J. Dudek and F.E. Close, *Phys. Lett.* **B583** (2004) 278.
- [34] C.E. Carlson *et al.*, [hep-ph/0312325](#).
- [35] R. N. Cahn and G. H. Trilling, *Phys. Rev.* **D69** (2004) 011501(R).
- [36] Q. Zhao and F. Close, [hep-ph/0404075](#).
- [37] CLAS Collaboration, H. G. Juengst, [nucl-ex/0312019](#).